

Compound Poisson Noise Sources in Diffusion-based Molecular Communication

Ali Etemadi [†], Paeiz Azmi [†], Hamidreza Arjmandi ^{*}, Nader Mokari [†]

[†] Tarbiat Modares University, ^{*} Yazd University

Abstract

Diffusion-based molecular communication (DMC) is one of the most promising approaches for realizing nano-scale communications for healthcare applications. The DMC systems in in-vivo environments may encounter biological organs that release molecules identical to the molecules used for signaling as part of their functionality. Such organs in the environment act as external noise source from the DMC system's perspective. Conventional simple receiver noise models are not able to characterize such external noise sources. In this paper, the release of molecules by biological noise sources is modeled as a compound Poisson process. The impact of compound Poisson noise sources (CPNSs) on the performance of a point-to-point DMC system is investigated. To this end, the noise from the CPNS observed at the receiver is characterized by exploiting the rare-event property of Poisson processes. Considering a simple on-off keying modulation and formulating maximum likelihood (ML) detector, the performance of DMC system in the presence of the CPNS is analyzed. For special case of CPNS in high-rate regime, the noise received from the CPNS is approximated as a Poisson process whose rate is normal distributed. It is proved that the distribution of noise from the CPNS in high-rate regime is log-concave and a simple single-threshold detector (STD) is optimal ML detector. Moreover, our results reveal that in general, adopting the conventional simple homogeneous Poisson noise model may lead to overly optimistic performance predictions, if a CPNS is present.

Index Terms– Diffusion-based molecular communication (DMC), biological organs, compound Poisson noise source (CPNS), compound Poisson process (CPP), maximum likelihood detector.

I. INTRODUCTION

A. Motivation

Diffusion based molecular communication (DMC) is a promising approach for realizing nano communications [1]. In DMC, information is encoded in the concentration, type, and/or release

time of molecules. In particular, a transmitter nanomachine releases information molecules into the environment. The released molecules move randomly via Brownian motion and, as a consequence, some molecules may be observed (received) at the receiver [2]. Specific features of DMC, such as its bio-compatibility, make it attractive for healthcare applications [3], [4]. However, the application of DMC systems in in-vivo environments faces many practical challenges and requires extensive research and development. Particularly, a realistic channel model is essential for the design of reliable DMC systems for in-vivo environments [5].

The biological organs in the body release different types of molecules as part of their functionality. The molecule release processes of biological organs exhibit a random behavior both for the time of release and the number of the released molecules. For instance, for the neuroendocrine system, the secretory bursts at random time instants have been modeled as a Poisson point process [6], [7]. As another example, the release of neurotransmitters in synapses has been characterized by a doubly stochastic Poisson process [8]. Also, the numbers of molecules transported by ion channels and ion pumps across the cell membrane can be stochastically modeled as Poisson random variables (RVs) [9]. DMC systems operating in in-vivo environments may encounter biological organs that release molecules identical to the molecules used for signaling. Such organs in the environment act as external noise sources from the DMC system's perspective. Therefore, accurate modeling of such noise sources taking into account their intrinsic characteristics is crucial for comprehensive performance analysis and evaluation.

B. Related Works

In the MC literature, different noise models have been proposed to characterize the uncertainty inherent to the molecule release process at the transmitter, Brownian motion, the reception process at the receiver, and environment noise. In [10], the noises introduced by the transmitter and the diffusion channel are modeled as additive Gaussian noise and are referred to as particle sampling and particle counting noise, respectively. In [11], it is shown that additive inverse Gaussian noise can be used to model the molecular timing channel where the information is encoded into the release time of the molecules into the fluid medium with drift. In [12], the authors propose a Poisson model to characterize the noise due to the randomness of the transmitter release process and the Brownian motion in the fluid medium. Also, in [13], additive stable distribution noise is introduced to characterize molecular timing channel for different modulation schemes.

The authors in [14] consider the continuous collision of molecules as source of noise leading to uncertainty in the position of the molecules. To mathematically model this noise source, the Langevin model for Brownian motion in a fluid medium is considered. The uncertainty caused by the reception process of ligand receptors is considered in [15]- [17]. Unlike for the noise introduced by the transmitter release, Brownian motion, and the reception process, less considerations has been given to the environmental noise in the DMC systems. The authors of [12] model environmental noise by a homogeneous Poisson distribution whose parameter is equal to the average number of molecules received during a given time slot. The homogeneous Poisson noise model is more elaborately presented in [18] where the dependence of the average number of noise molecules, i.e., the parameter of the distribution, on the time-slot duration is taken into account. However, these conventional noise models which are homogeneous in space and time are not capable of accurately modeling the noise introduced by biological organs, which is the main focus of this paper.

C. Proposed Model

Our proposed model provides a general framework for analyzing the performance of DMC systems in the presence of biological noise sources. To the best of our knowledge, this is the first work to investigate the impact of the probabilistic nature of the molecule release time instances of external sources on the performance of DMC systems. As a realistic assumption in in-vivo environments, external noise sources which release molecules has not been adopted in existing literature. Considering an external biological noise source releasing random numbers of molecules in random time instances leads to receiver noise whose statistics differ from that of the conventional noise models. In other words, conventional noise models are not able to model the noise caused by biological organs. In this paper, a point-to-point DMC system is considered in the presence of an external noise source which releases molecules of the same type as the signaling molecules. Inspired by the molecule release of biological organs [6], [7], the release process of the noise source is modeled as a compound Poisson process (CPP) where the release time events constitute points of a Poisson process and the amplitudes of the events (the number of released molecules at a release time event) are random. Such an external noise source is referred to as a compound Poisson noise source (CPNS) in the following. The CPNS takes into account the randomness of the release events of biological organs in both time and amplitude. To

investigate the impact of CPNS on communication performance, a point-to-point DMC system with simple on-off keying modulation is considered. The number of noise molecules observed at the receiver is analyzed and approximated by a Poisson mixture distribution by using the rare-event property of Poisson distributions. Considering a simple on-off keying modulation, the performance of DMC system in the presence of CPNS is analyzed. A symbol-by-symbol maximum likelihood (ML) detector is derived and bit error rate (BER) is obtained by adopting a simple single-threshold detector (STD). For the special case of CPNS in high-rate regime (high rates of release time events), the noise received from the CPNS is approximated as a Poisson distribution whose mean is normal distributed. It is proved that the noise received from the CPNS in high-rate regime has a log-concave distribution and a STD is optimal ML detector. For the general case of CPNS, our results report that the distribution of noise received from the CPNS may not be log-concave and can even be multimodal distribution leading to optimality of multiple-threshold detector (not a simple STD). Moreover, our simulation results confirm the obtained analytical BER expressions. Also, it is revealed that the conventional homogeneous Poisson noise model is not applicable to CPNSs and leads to overly optimistic performance estimates.

The remainder of this paper is organized as follows: In Section II, we present the DMC system model including the transmitter, receiver, channel, and CPNS models. In Section III, the distributions of the received signals due to the release of molecules by the transmitter and the CPNS are derived. The optimal ML detector and the error probability of the DMC system in the presence of a CPNS are analyzed in Section IV. In Section V, we provide simulation and numerical results. Finally, the paper is concluded in Section VI.

II. SYSTEM MODEL

A point-to-point DMC system is considered in the presence of a CPNS. It is assumed that the receiver is at the origin of the coordinate system and is synchronized with the transmitter [19]. The transmitter and the CPNS are assumed to be point sources, located at distances of d_T and d_C from the receiver, respectively; see Fig. ?? . The signaling molecules and the noise molecules released by the transmitter and the CPNS, respectively, are of the same type A . Simple on-off keying modulation with time-slot duration T is adopted where bits 1 and 0 are represented by the release of N molecules (on average) and no molecule at the beginning of each time slot,

respectively. Assuming transmission of bit 1, the number of molecules released by the transmitter follows a Poisson distribution with mean N [12]. The receiver is assumed to be a transparent spherical volume of radius r_R that counts the number of molecules inside the receiver volume at sampling time t_s [20]. The receiver uses the observed sample to decide about the transmitted bit. In the rest of this section, the CPNS model is presented and the adopted channel model is described.

A. CPNS Model

We propose a general CPP model for an external bio-inspired noise source in in-vivo environments. The resulting CPNS models the randomness of the molecule release process both in time and amplitude. A general CPP or space-time Poisson process is defined as follows [21]:

Definition 1. Let $N(t)$ denote a Poisson process characterized by RV $n_e(t, u_t)$ representing the event arrival rate of distribution family $u_t \in U$ at time t . Also, let RV $Q(t, w_t)$ denote the time-dependent amplitudes due to a corresponding event at time t from the distribution family $w_t \in W$. Then, a general CPP is defined as the sum of the event amplitudes up to time t and is given by

$$\Pi(t) = \int_0^t Q(\tau, w_\tau) n_e(\tau, u_\tau) d\tau. \quad (1)$$

In particular, the molecule release times of the CPNS are modeled as a Poisson point process with rate $n_e(t, u_t)$ and the number of molecules released at a release event, $Q(t, w_t)$, is also a RV, which may follow some time-dependent distribution. This model is inspired by the release processes observed in biological organs, such as secretory bursts in the neuroendocrine system [6], [7] and the release of neurotransmitters in synapses [8].

In [6], [7], the authors model the release process of secretory bursts by superimposing the random burst amplitudes on a Poisson process representing the timing of the secretory burst events. The authors aim is to provide a mathematical model for neurohormone secretion for physiological investigations. Considering Definition 1, this model for secretory bursts constitutes a CPP, regardless of the release amplitude distribution. The release of neurotransmitters in synapses has been modeled as a doubly stochastic Poisson process in [8]. A doubly Poisson

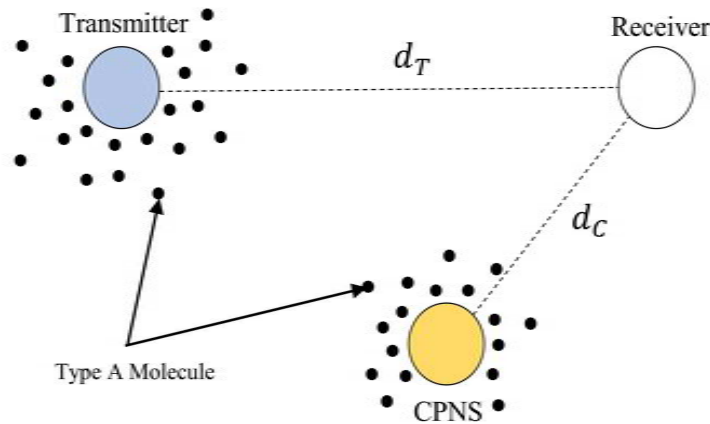


Fig. 1. Comparison of BERs (exact, approximation, and simulation) versus time interval \tilde{T} for different values of λ_e .

process is a Poisson process with a random arrival rate. Hence, according to Definition 1, regardless of the distribution of the release amplitudes, doubly Poisson process is a CPP.

We assume that the CPNS follows a special CPP where the Poisson point process representing the release times has a fixed rate of λ_e . This simplifying assumption is justified based on the slow variation of biological processes modulating the release rate of CPNS compared to the transmission time slot duration of DMC systems (usually in the order of seconds). Moreover, the release amplitude (the number of molecules released at the release time of the CPNS) is assumed to be a Poisson RV with parameter λ_a . This assumption is confirmed in [9] where the authors show that the number of molecules released by ion channels and ion pumps over the cell membrane are Poisson distributed. For better perception of the logic behind this assumption, consider a chamber including large number of molecules. If each molecule has a small probability to exit during a time interval, the total number of exiting molecules is Poisson distributed RV with mean of the average exiting molecules during the time interval. In summary, we assume a CPNS with the Poisson point process representing the release times of the fixed rate of λ_e where the release event amplitudes are assumed mutually independent and identical Poisson RVs, independent from the Poisson point process of the release time events.

B. Channel Model

In the considered DMC system, the transmitter and the CPNS release molecules into the environment. The molecules diffuse following a Brownian motion and their movements are assumed to be independent of each other. The concentration of molecules of type A having

diffusion coefficient D at location $\mathbf{r} = (x, y, z)$ and time t , $C(\mathbf{r}, t)$, is characterized by Fick's second law as follows [22]:

$$\frac{\partial C(\mathbf{r}, t)}{\partial t} = D \nabla^2 C(\mathbf{r}, t), \quad (2)$$

where ∇^2 is the Laplacian operator. We assume an impulsive point source molecule release $\delta(\mathbf{r}, t) = \delta(x)\delta(y)\delta(z)\delta(t)$ into an unbounded 3-dimensional environment, where $\delta(\cdot)$ denotes the well-known Dirac delta function. Solving (2), concentration $C(\mathbf{r}, t)$ is obtained as follows:

$$C(\mathbf{r}, t) = \frac{1}{(4\pi Dt)^{3/2}} \exp\left(-\frac{r^2}{4Dt}\right) u(t), \quad (3)$$

where $r = (x^2 + y^2 + z^2)^{1/2}$ and $u(t)$ is step function. Thereby, the expected number of molecules observed by a transparent spherical receiver with volume $V_R = \frac{4}{3}\pi r_R^3$, whose center is at a distance of r from the source, can be approximated as [23]:

$$p(t) = \frac{V_R}{(4\pi Dt)^{3/2}} \exp\left(-\frac{r^2}{4Dt}\right) u(t). \quad (4)$$

The impulsive input $\delta(\mathbf{r}, t)$ can be interpreted as the release of a single molecule at the origin, $\mathbf{r} = (0, 0, 0)$, and at time $t = 0$. Correspondingly, $p(t)$ in (4) represents the probability that the released molecule is observed inside the receiver at time t . It is obvious from (3) that the DMC channel has memory, i.e., a molecule released at the beginning of the current time slot may not be observed at the receiver in the current time slot but may be observed in one of the next time slots. Theoretically, the DMC channel has infinite memory, since $C(\mathbf{r}, t)$ given in (3) has an infinite tail. However, from a practical perspective, a finite channel memory can be assumed [24]. To this end, we define the channel memory as the time it takes until a released molecule arrives at the receiver with a high probability. A probability of 0.95 is adopted in this paper, i.e., we have

$$\int_{\tau=0}^{t_m} C(\mathbf{r}, t) d\tau = 0.95 \int_{\tau=0}^{\infty} C(\mathbf{r}, t) d\tau, \quad (5)$$

where t_m denotes the channel memory in seconds. Correspondingly, $k = \lfloor t_m/T \rfloor$ is the channel memory in terms of the number of time slots where $\lfloor x \rfloor$ denotes the largest integer less than or equal to x . Obviously, the distances between transmitter and receiver (d_T) and between CPNS and receiver (d_C) affect the respective channel memories which are denoted by k_T and k_C ,

respectively.

III. RECEIVED SIGNAL AT THE RECEIVER

In order to investigate the performance of the considered DMC system, the received signal has to be characterized. In other words, the distribution of the number of molecules observed at the receiver at sampling time t_s has to be obtained. The molecules observed at the receiver originate from two independent sources, namely the transmitter and the CPNS. In this section, we derive the distributions of the numbers of molecules received from the transmitter and the CPNS, respectively. Specifically, the rare-event property of the Poisson process is employed to obtain a simplified closed-form expression for distribution of the noise received from CPNS. Also, for the special case of CPNS in high-rate regime, the noise received from the CPNS is approximated by a Poisson process whose rate is normal distributed.

A. Signal Received from Transmitter

Let $B_0 \in \{0, 1\}$ and $B_j \in \{0, 1\}, j = 1, 2, \dots, k_T$, denote the RVs representing the bits transmitted in the current time slot and the j^{th} previous time slot, respectively. Based on the system model described in Section II, to transmit bit B_j , the transmitter releases X_j molecules at the beginning of the j^{th} time slot where $X_j|B_j = b_j \sim \text{Poisson}(b_j N)$. In other words, if $B_j = 0$, no molecule is released and if $B_j = 1$, the number of released molecules is Poisson distributed with parameter N . A molecule released at the beginning of the j^{th} , $j = 0, 1, \dots, k_T$, time slot is observed at the receiver at sampling time t_s of the current time slot with probability $p_T(jT + t_s)$, where $p_T(t)$ is given in (4) after substituting r by d_T . Based on the thinning property of the Poisson distribution [25], the number of molecules received at the receiver due to transmission of $B_0 = b_0$ in the current time slot, Y_T^c , is Poisson distributed with mean $Nb_0p_T(t_s)$, i.e.,

$$p_{Y_T^c}[k|B_0 = b_0] = \exp\left(-Nb_0p_T(t_s)\right) \frac{\left(Nb_0p_T(t_s)\right)^k}{k!}, \quad k = 0, 1, 2, \dots \quad (6)$$

Similarly, the number of molecules observed at the receiver in the current time slot due to transmission of $B_j = b_j$ in the j^{th} previous time slot is Poisson distributed with parameter $Nb_jp_T(jT + t_s)$, i.e., $Y_T^j|B_j = b_j \sim \text{Poisson}\left(Nb_jp_T(jT + t_s)\right)$. The number of molecules

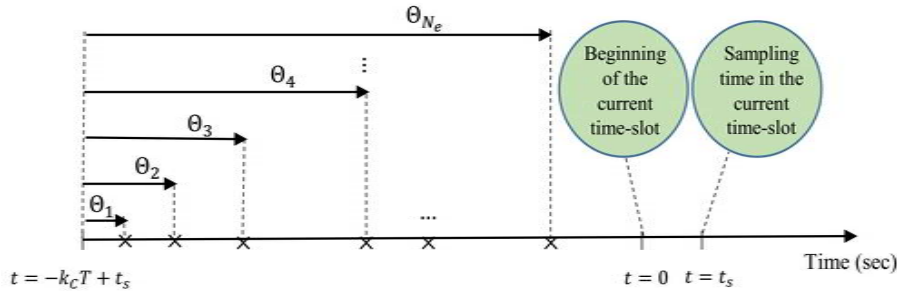


Fig. 2. Comparison of BERs (exact, approximation, and simulation) versus time interval \tilde{T} for different values of λ_e .

observed at the receiver in the current time slot due to transmission of all previous bits (interference) equals $Y_T^I = \sum_{j=1}^{k_T} Y_T^j$. Given the previous transmitted bits $B_j = b_j, j = 1, 2, \dots, k_T$, the $Y_T^j, j = 1, \dots, k_T$, are independent and Y_T^I follows a Poisson distribution with mean $N \sum_{j=1}^{k_T} b_j p_T(jT + t_s)$, i.e., we have:

$$p_{Y_T^I}[k | \mathbf{B}_{1:k_T} = \mathbf{b}_{1:k_T}] = \exp \left(-N \sum_{j=1}^{k_T} b_j p_T(jT + t_s) \right) \frac{\left(N \sum_{j=1}^{k_T} b_j p_T(jT + t_s) \right)^k}{k!}, \quad k = 0, 1, 2, \dots, \quad (7)$$

where $\mathbf{B}_{1:k_T} = [B_1, B_2, \dots, B_{k_T}]$, $\mathbf{b}_{1:k_T} = [b_1, b_2, \dots, b_{k_T}]$, and the notation $\mathbf{A}_{i:k}$ denotes vector $[A_i, A_{i+1}, \dots, A_k]$.

B. Noise Received from CPNS

The memory of the channel between the CPNS and the receiver is k_C time slots. Considering the CPNS Poisson point process of release events with rate λ_e , the number of release events in the k_C previous time slots, $k_C T$, denoted by $N_e(k_C T)$, is a Poisson RV with mean $\lambda_e k_C T$. For ease of notation, in the rest of the paper, we denote $N_e(k_C T)$ by N_e . The time elapsed since the time instant $-k_C T + t_s$ until the i^{th} release event is denoted by Θ_i ; see Fig. ???. Hence, the i^{th} release event occurs at time $-k_C T + t_s + \Theta_i$.

Given the release of a molecule by the CPNS at time 0, the probability of observing this molecule at the receiver is $p_C(t)$, given by (4) after substituting r by d_C . The release amplitude of the i^{th} event is Poisson distributed with parameter λ_a . Therefore, based on the thinning property of the Poisson distribution, the number of molecules observed at the receiver due to the i^{th} release event of the CPNS, Y_C^i , is Poisson distributed with mean $\lambda_a p_C(k_C T - \theta_i)$ for

$\Theta_i = \theta_i$, i.e.,

$$Y_C^i | \Theta_i = \theta_i \sim \text{Poisson}(\lambda_a p_C(k_C T - \theta_i)). \quad (8)$$

The total number of molecules observed at the receiver in the current time slot (at time $t = t_s$) due to the molecule release by the CPNS during the k_C previous time slots is equal to $Y_C = \sum_{i=1}^{k_C} Y_C^i$. Assuming $N_e = n$, i.e., the number of release events in the k_C previous time slots is equal to n and $\Theta_{1:n} = \theta_{1:n}$, Y_C follows a Poisson distribution with parameter $\lambda_a \sum_{i=1}^n p_C(k_C T - \theta_i)$. Therefore, we can write

$$\begin{aligned} p_{Y_C}[k] &= \sum_{n=0}^{\infty} \int_{\theta_{1:n}} p_{Y_C}[k | N_e = n, \Theta_{1:n} = \theta_{1:n}] f_{\Theta_{1:n}}(\theta_{1:n} | N_e = n) p_{N_e}[n] d\theta_{1:n} \\ &= \sum_{n=0}^{\infty} \int_{\theta_{1:n}} \exp\left(-\lambda_a \sum_{i=1}^n p_C(k_C T - \theta_i)\right) \frac{\left(\lambda_a \sum_{i=1}^n p_C(k_C T - \theta_i)\right)^k}{k!} f_{\Theta_{1:n}}(\theta_{1:n} | N_e = n) p_{N_e}[n] d\theta_{1:n}, \end{aligned} \quad (9)$$

where $p_{Y_C}[\cdot]$ denotes the distribution of RV Y_C , the Θ_i s are points of a Poisson process, N_e is the RV representing the total number of release events occurring during $[-k_C T + t_s, t_s]$, respectively. Also, $f_{\Theta_{1:n}}(\theta_{1:n} | N_e = n)$ is the joint pdf of release time events $\Theta_{1:n}$ given n events, and $d\theta_{1:n}$ stands for $d\theta_1 d\theta_2 \cdots d\theta_n$. Since the points of a Poisson process, $\Theta_{1:n}$, form a Markov chain [26], we have:

$$\begin{aligned} f_{\Theta_{1:n}}(\theta_{1:n} | N_e = n) &= \prod_{i=1}^n f_{\Theta_i}(\theta_i | \theta_{i-1}, N_e = n) \\ &= f_{\Theta_1}(\theta_1 | N_e = n) f_{\Theta_2}(\theta_2 | \theta_1, N_e = n) \cdots f_{\Theta_n}(\theta_n | \theta_{n-1}, N_e = n). \end{aligned} \quad (10)$$

The time difference between two events of a Poisson process is exponentially distributed, which leads to:

$$f_{\Theta_i}(\theta_i | \theta_{i-1}, N_e = n) = \lambda_e e^{-\lambda_e(\theta_i - \theta_{i-1})} u(\theta_i - \theta_{i-1}), \quad (11)$$

where $u(\cdot)$ denotes the unit step function. Therefore, (10) reduces to

$$f_{\Theta_{1:n}}(\theta_{1:n} | N_e = n) = \lambda_e^n e^{-\lambda_e \theta_n} u(\theta_n - \theta_{n-1}). \quad (12)$$

Substituting $p_{N_e}[n] = e^{-\lambda_e k_C T} (\lambda_e k_C T)^n / n!$ and applying (12) in (9), we have:

$$\begin{aligned}
 p_{Y_C}[k] &= \sum_{n=0}^{\infty} \int_{\theta_{1:n}} \exp \left(-\lambda_a \sum_{i=1}^n p_C(k_C T - \theta_i) \right) \frac{\left(\lambda_a \sum_{i=1}^n p_C(k_C T - \theta_i) \right)^k}{k!} \lambda_e^n e^{-\lambda_e \theta_n} \exp(-\lambda_e k_C T) \frac{(\lambda_e k_C T)^n}{n!} d\theta_{1:n}.
 \end{aligned} \tag{13}$$

Generally, obtaining a closed-form expression for the above integral is cumbersome. In the next subsection, the rare-event property [27] of the Poisson process is employed to obtain a simplified closed-form expression for $p_{Y_C}[k]$.

C. Rare Event Based Analysis of the Noise Received from the CPNS

The rare event property of a Poisson process with parameter λ states that the probability of occurrence of an event in a short time interval Δt ($\Delta t \ll 1/\lambda$) is proportional to the duration of the interval, i.e., $\lambda \Delta t$. Also, for sufficiently small Δt , the probability of occurrence of more than one event is negligible. As a result, the probability of no event occurring in this interval is equal to $1 - \lambda \Delta t$ [25], [27].

For a sufficiently short time interval \tilde{T} , such that $\lambda_e \tilde{T} \ll 1$, the rare event property holds. Given \tilde{T} , the channel memory duration, $k_C T$, can be divided into $\tilde{k}_C = \frac{k_C T}{\tilde{T}}$ distinct time intervals of length \tilde{T} . Let \tilde{Y}_C^i denote the number of molecules received in the current time slot due to the release event of the CPNS in the i^{th} , $i = 1, \dots, \tilde{k}_C$, previous short time interval, $[-(\tilde{k}_C - i + 1)\tilde{T} + t_s, -(\tilde{k}_C - i)\tilde{T} + t_s]$. Therefore, the total number of molecules received from the CPNS in the current time slot is $Y_C = \sum_{i=1}^{\tilde{k}_C} \tilde{Y}_C^i$. Because of the independence of the release time instants in distinct intervals for a Poisson process, the \tilde{Y}_C^i are mutually independent, and we have

$$p_{Y_C}[k] = p_{\tilde{Y}_C^1}[k] \otimes p_{\tilde{Y}_C^2}[k] \otimes \dots \otimes p_{\tilde{Y}_C^{\tilde{k}_C}}[k], \tag{14}$$

where \otimes is the convolution operator and $p_{\tilde{Y}_C^i}[k]$ denotes the distribution of the number of molecules received in the current time slot due to the release event of the CPNS in the i^{th} , $i = 1, \dots, \tilde{k}_C$, previous short time interval.

In the i^{th} previous short time interval, no molecule is released with probability $1 - \lambda_e \tilde{T}$. If no molecule is released, which we refer to as event \mathcal{F}_0^i , no molecule is observed at the receiver, i.e., $p_{\tilde{Y}_C^i}[k|\mathcal{F}_0^i] = \delta[k]$. Otherwise, one event occurs in the i^{th} short time interval at time t_i ,

$t_i \in [-(\tilde{k}_C - i + 1)\tilde{T} + t_s, -(\tilde{k}_C - i)\tilde{T} + t_s]$, which can be modeled as a uniform RV, since the time interval is short and includes only one occurrence. Defining $\tilde{\Theta}_i = t_i + \tilde{k}_C\tilde{T} - t_s$ (the time elapsed since time instant $-\tilde{k}_C\tilde{T} + t_s$ until the release event at t_i), $\tilde{\Theta}_i$ is a uniform RV in interval $[(i - 1)\tilde{T}, i\tilde{T}]$, correspondingly. Thereby, given one event occurrence, \mathcal{F}_1^i , and the occurrence time $\tilde{\Theta}_i = \tilde{\theta}_i$, the number of molecules received in the current time slot follows a Poisson distribution with parameter $\mu(\tilde{\Theta}_i) = \lambda_a p_C(k_C T - \tilde{\Theta}_i)$, i.e.,

$$p_{\tilde{Y}_C^i}[k|\mathcal{F}_1^i] = \int_{(i-1)\tilde{T}}^{i\tilde{T}} p_{\tilde{Y}_C^i}[k|\mathcal{F}_1^i, \tilde{\theta}_i] \frac{1}{\tilde{T}} d\tilde{\theta}_i = \int_{(i-1)\tilde{T}}^{i\tilde{T}} e^{-\mu(\tilde{\theta}_i)} \frac{(\mu(\tilde{\theta}_i))^k}{k!} \frac{1}{\tilde{T}} d\tilde{\theta}_i, \quad i = 1, 2, \dots, \tilde{k}_C. \quad (15)$$

Therefore, we obtain

$$\begin{aligned} p_{\tilde{Y}_C^i}[k] &= p_{\tilde{Y}_C^i}[k|\mathcal{F}_0^i]p(\mathcal{F}_0^i) + p_{\tilde{Y}_C^i}[k|\mathcal{F}_1^i]p(\mathcal{F}_1^i) \\ &= (1 - \lambda_e \tilde{T})\delta[k] + (\lambda_e \tilde{T})p_{\tilde{Y}_C^i}[k|\mathcal{F}_1^i], \quad i = 1, 2, \dots, \tilde{k}_C, \end{aligned} \quad (16)$$

where $p_{\tilde{Y}_C^i}[k|\mathcal{F}_1^i]$ is given by (15). To simplify the notation, we employ $f_i[k] = p_{\tilde{Y}_C^i}[k|\mathcal{F}_1^i]$ in the rest of the paper. Eq. (14) can be simplified as follows, see Appendix A,

$$p_{Y_C}[k] = \sum_{i=0}^{\tilde{k}_C} (1 - \lambda_e \tilde{T})^{\tilde{k}_C - i} (\lambda_e \tilde{T})^i \sum_{h=1}^{\mathfrak{K}_i} \delta[k] \otimes f_{\alpha_1^h}[k] \otimes \dots \otimes f_{\alpha_i^h}[k], \quad (17)$$

where $\mathfrak{K}_i \triangleq \binom{\tilde{k}_C}{i}$ is the number of i -element subsets of set $\{1, 2, \dots, \tilde{k}_C\}$, and the elements of the h^{th} i -element subset are denoted by $\alpha_1^h, \dots, \alpha_i^h$. The distribution in (17) is complicated and does not have a closed form expression when the exact distribution of $p_{\tilde{Y}_C^i}[k]$ given in (15) is employed which is referred to as rare-event exact distribution for the noise received from the CPNS. To obtain a closed form expression, we approximate $p_{\tilde{Y}_C^i}[k|\mathcal{F}_1^i]$ as a Poisson distribution with a fixed mean. Since $\tilde{\Theta}_i$ is a uniform RV in interval $[(i - 1)\tilde{T}, i\tilde{T}]$, by adopting sufficiently small \tilde{T} ($\tilde{T} \ll k_C T$), $k_C T - (i - 1)\tilde{T}$, very closely approximates $k_C T - \tilde{\Theta}_i$. Therefore, we can approximate the mean $\mu(\tilde{\Theta}_i)$ as follows

$$\mu(\tilde{\Theta}_i) = \lambda_a p_C(k_C T - \tilde{\Theta}_i) \simeq \lambda_a p_C(k_C T - (i - 1)\tilde{T}) \triangleq \mu_i, \quad i = 1, 2, \dots, \tilde{k}_C, \quad (18)$$

which leads to $f_i[k] = p_{\tilde{Y}_C^i}[k|\mathcal{F}_1^i] \cong e^{-\mu_i} \frac{(\mu_i)^k}{k!}$. Thereby, the convolution term in (17) is reduced to

$$f_{\alpha_0^h}[k] \otimes f_{\alpha_1^h}[k] \otimes \cdots \otimes f_{\alpha_i^h}[k] \cong \exp\left(-\sum_{l=0}^i \mu_{\alpha_l^h}\right) \frac{(\sum_{l=0}^i \mu_{\alpha_l^h})^k}{k!}, \quad (19)$$

and hence

$$p_{Y_C}[k] = \sum_{i=0}^{\tilde{k}_C} (1 - \lambda_e \tilde{T})^{\tilde{k}_C - i} (\lambda_e \tilde{T})^i \sum_{h=1}^{\mathfrak{R}_i} \exp\left(-\sum_{l=0}^i \mu_{\alpha_l^h}\right) \frac{(\sum_{l=0}^i \mu_{\alpha_l^h})^k}{k!}, \quad (20)$$

which is a Poisson mixture distribution [28], i.e., $p_{Y_C}[k]$ is a summation of weighted Poisson distributions where the sum of the weights is equal to 1, since

$$\sum_{i=0}^{\tilde{k}_C} (1 - \lambda_e \tilde{T})^{\tilde{k}_C - i} (\lambda_e \tilde{T})^i \mathfrak{R}_i = 1. \quad (21)$$

We refer to the approximation in (20) as rare-event approximate distribution for noise received from the CPNS. Our simulation results demonstrate that the rare-event approximate analysis very closely approaches the rare-event exact analysis in (17) for small values of \tilde{T} .

D. Noise Received from the CPNS in the High-rate Regime

From Subsection III-B, the number of molecules received from the CPNS at the current time slot follows a Poisson distribution with random rate $M = \lambda_a \sum_{i=1}^{N_e} p_C(k_C T - \Theta_i)$ where N_e is a RV denoting the number of release events during the k_C previous time slots and Θ_i denotes a RV representing the release time of the i^{th} event with respect to the beginning of the k_C^{th} previous time slot. Defining stochastic process $\mathbf{M}(t) = \sum_{i=1}^{N_e} \lambda_a p_C(t - \Theta_i)$, we can write $M = \mathbf{M}(k_C T)$. The $\mathbf{M}(t)$ can be interpreted as a shot-noise process passed over a linear time invariant (LTI) system with impulse response $\lambda_a p_C(t)$ [32]- [33], i.e.,

$$\mathbf{M}(t) = \sum_{i=-\infty}^{+\infty} \delta(t - \Theta_i) \otimes \lambda_a p_C(t), \quad (22)$$

where $p_C(t)$ is given in (4) and Θ_i s are points of a Poisson process with rate λ_e ¹. The cumulants of a shot-noise process passing from an LTI system with impulse response $h(t)$ are time invariant

¹Since we have $p_C(t) = 0$ for $t < 0$ and $t > k_C T$, inclusion of $\Theta_i < 0$ or $\Theta_i > k_C T$ in the summation of $\mathbf{M}(t) = \sum_{i=1}^{N_e} \lambda_a p_C(t - \Theta_i)$ is allowed and equivalently we can write $\mathbf{M}(t) = \sum_{i=-\infty}^{+\infty} \lambda_a p_C(t - \Theta_i)$

which are given by [33]:

$$k_n = \lambda_e \int_{-\infty}^{+\infty} h^n(\tau) d\tau, \quad \forall n \geq 1. \quad (23)$$

Thereby, this process is a first order strict sense stationary (SSS) process whose first order distribution function is time independent. The authors in [32] show that for high values of λ_e ($\lambda_e \rightarrow \infty$), the first order distribution of this process approaches a Gaussian distribution with mean k_1 and variance k_2 given in (23). Considering $h(t) = \lambda_a p_C(t)$ where $p_C(t)$ is given in (4), the cummulants of $\mathbf{M}(t)$ are obtained as follows

$$k_n = \frac{1}{n} G_1 G_2^n \Gamma\left(\frac{3n}{2} - 1, \frac{nd_C^2}{4Dk_C T}\right), \quad \forall n \geq 1, \quad (24)$$

where $G_1 = \frac{\lambda_e d^2}{4D}$, $G_2 = \frac{\lambda_a V_R}{\pi^{3/2} d_C^3}$, and $\Gamma(s, x) = \int_x^\infty t^{s-1} e^{-t} dt$ denotes the upper incomplete Gamma function. Therefore, for CPNS in a high-rate regime (large values of λ_e), ($\lambda_e \rightarrow \infty$), M follows a Gaussian distribution with mean k_1 and variance k_2 given in (24), i.e.,

$$f_M(m) = (2\pi k_2)^{1/2} \exp\left(-\frac{(m - k_1)^2}{2k_2}\right), \quad (25)$$

As a result, the number of molecules received from the CPNS in high rate regime, Y_C , follows a Poisson distribution with parameter $M \sim \mathcal{N}(k_1, k_2)$, and we can write:

$$p_{Y_C}[k] = \int_0^{+\infty} p_{Y_C}[k|m] f_M(m) dm. \quad (26)$$

In Appendix B, we obtain the following closed form expression for $p_{Y_C}[k]$

$$p_{Y_C}[k] = l(k_1, k_2) k_2^{(k+1)/2} D_{-k-1}\left(\sqrt{k_2}\left(1 - \frac{k_1}{k_2}\right)\right), \quad (27)$$

where

$$l(k_1, k_2) \triangleq (2\pi k_2)^{-1/2} \exp(-k_1^2/2k_2 + k_2(1 - \frac{k_1}{k_2})^2/4), \quad (28)$$

and $D_\nu(z)$ is the parabolic cylinder function which is defined as follows

$$D_\nu(z) \triangleq 2^{\nu/2} e^{-z^2/4} \left[\frac{\sqrt{\pi}}{\Gamma(\frac{1-\nu}{2})_1} F_1\left(-\frac{\nu}{2}, \frac{1}{2}; \frac{z^2}{2}\right) - \frac{\sqrt{2\pi}z}{\Gamma(-\frac{\nu}{2})_1} F_1\left(\frac{1-\nu}{2}, \frac{3}{2}; \frac{z^2}{2}\right) \right], \quad (29)$$

in which ${}_1F_1(\alpha, \gamma; z)$ denotes the confluent hypergeometric function as follows:

$${}_1F_1(\alpha, \gamma; z) = \sum_{n=0}^{+\infty} \frac{\Gamma(\alpha+n)\Gamma(\gamma)}{\Gamma(\alpha)\Gamma(\gamma+n)} \frac{z^n}{n!}. \quad (30)$$

where $\Gamma(\cdot)$ denotes the Gamma function.

IV. ERROR PROBABILITY ANALYSIS

In Section III, the signal received from the transmitter, Y_T , and the noise received from the CPNS, Y_C , were analyzed. In this section, we analyze the performance of a point-to-point DMC link in the presence of a CPNS in terms of the BER. The total received signal at the receiver is given by

$$Y = Y_T + Y_C = Y_T^c + Y_T^I + Y_C, \quad (31)$$

where Y_T^c is the signal received in the current time slot due to the current transmission and Y_T^I is the interference received in the current time slot originating from transmissions in previous time slots. Y_T^c and Y_T^I are independent Poisson-distributed RVs with parameters $Nb_0p_T(t_s)$ and $N \sum_{j=1}^{k_T} b_j p_T(jT + t_s)$, given $B_0 = b_0$ and $\mathbf{B}_{1:k_T} = \mathbf{b}_{1:k_T}$, respectively. In order to focus on the impact of the CPNS on the performance, we assume the receiver employs the mean of the previous transmitted bits, i.e., $Y_T^I \sim \text{Poisson}(\frac{N}{2} \sum_{j=1}^{k_T} p_T(jT + t_s))$, by assuming symmetric input, i.e., $\Pr(B_j = 0) = \Pr(B_j = 1) = \frac{1}{2}, \forall j \in \{1, 2, \dots, k_T\}$. Thereby, $Y_T = Y_T^c + Y_T^I$ follows a Poisson distribution with parameter $NB_0p_T(t_s) + \frac{N}{2} \sum_{j=1}^{k_T} p_T(jT + t_s)$, i.e.,

$$\begin{aligned} p_{Y_T}[k|B_0 = b_0] \\ = \exp\left(-Nb_0p_T(t_s) - \frac{N}{2} \sum_{j=1}^{k_T} p_T(jT + t_s)\right) \frac{\left(Nb_0p_T(t_s) + \frac{N}{2} \sum_{j=1}^{k_T} p_T(jT + t_s)\right)^k}{k!}. \end{aligned} \quad (32)$$

The noise received from the CPNS, Y_C , is a Poisson mixture given by (20). Therefore, conditioned on transmitted bit in the current time slot, the total number of molecules observed at the receiver also follows a Poisson mixture distribution as follows:

$$p_Y[k|B_0 = b_0] = \sum_{i=0}^{\tilde{k}_C} (1 - \lambda_e \tilde{T})^{\tilde{k}_C - i} (\lambda_e \tilde{T})^i \sum_{h=1}^{\mathfrak{R}_i} e^{-v_i^h(b_0)} \frac{\left(v_i^h(b_0)\right)^k}{k!}, \quad (33)$$

where $v_i^h(b_0) = Nb_0p_T(t_s) + \frac{N}{2} \sum_{j=1}^{k_T} p_T(jT + t_s) + \sum_{l=0}^i \mu_{\alpha_l^h}$.

Receiving $Y = y$ molecules in the current time slot, a symbol-by-symbol ML detector selects

$$\hat{B}_0 = \underset{b_0}{\operatorname{argmax}} p_Y[y|B_0 = b_0], \quad (34)$$

where \hat{B}_0 denotes the estimated transmitted bit in the current time slot.

Generally, the optimal ML detector (34) is a MTD which is characterized by m threshold values, $\zeta_1, \zeta_2, \dots, \zeta_m$ partitioning feasible observation space ($y \in \mathbb{R}_+$) and the decisions on the transmitted bit based on the observed y in all disjoint partitions determined by the threshold values. For nanomachines, which have limited resources, STDs ($m = 1$) are desirable. An STD, denoted by $\Phi(y)$, is characterized as follows:

$$\Phi(y) = \begin{cases} 0 & y < \zeta \\ 1 & y \geq \zeta \end{cases}, \quad (35)$$

where y is the observation and ζ is the decision threshold.

Given a STD with threshold value ζ , the BER of the system is obtained as follows:

$$\begin{aligned} P_e &= \frac{1}{2} \Pr(\hat{B}_0 = 1|B_0 = 0) + \frac{1}{2} \Pr(\hat{B}_0 = 0|B_0 = 1) \\ &= \frac{1}{2} \Pr(y \geq \zeta|B_0 = 0) + \frac{1}{2} \Pr(y < \zeta|B_0 = 1) \\ &= \frac{1}{2} \left(1 - \mathcal{F}_Y(\zeta|B_0 = 0) \right) + \frac{1}{2} \mathcal{F}_Y(\zeta|B_0 = 1), \end{aligned} \quad (36)$$

where $\mathcal{F}_Y(\cdot)$ denotes the cumulative distribution function (CDF) of RV Y .

Considering the distribution of received signal given by (33), the BER terms $\Pr(\hat{B}_0 = 1|B_0 = 0)$ and $\Pr(\hat{B}_0 = 0|B_0 = 1)$ in (36) are calculated as follows:

$$\begin{aligned} \Pr(\hat{B}_0 = 1|B_0 = 0) &= \Pr(y > \zeta|B_0 = 0) \\ &= \sum_{i=0}^{\tilde{k}_C} (1 - \lambda_e \tilde{T})^{\tilde{k}_C - i} (\lambda_e \tilde{T})^i \sum_{h=1}^{\tilde{\kappa}_i} \left(1 - \frac{\Gamma(\zeta, v_i^h(b_0 = 0))}{\Gamma(\zeta)} \right), \end{aligned} \quad (37)$$

$$\begin{aligned} \Pr(\hat{B}_0 = 0|B_0 = 1) &= \Pr(y \leq \zeta|B_0 = 1) \\ &= \sum_{i=0}^{\tilde{k}_C} (1 - \lambda_e \tilde{T})^{\tilde{k}_C - i} (\lambda_e \tilde{T})^i \sum_{h=1}^{\tilde{\kappa}_i} \frac{\Gamma(\zeta, v_i^h(b_0 = 1))}{\Gamma(\zeta)}, \end{aligned} \quad (38)$$

where $\Gamma(\delta, \sigma)$ is the incomplete Gamma function given by $\Gamma(\delta, \sigma) = \int_{\sigma}^{\infty} e^{-t} t^{\delta-1} dt$ and $\Gamma(\delta, \sigma)/\Gamma(\delta)$

denotes the CDF of the Poisson distribution with parameter σ .

A. On the Optimality of Single-Threshold Detector

In this subsection, we first prove that STD is optimal for CPNS in high-rate regime and then discuss on optimality of STD in general case.

Proposition 1. For the CPNS in the high-rate regime (large values of λ_e), the optimal ML detector (34) is a single-threshold detector.

Proof. The detector is supposed to detect the transmitted bit is 1 or 0 which is equivalent to the presence or absence of signal $\text{Poisson}(Np_T(t_s))$ which is embedded in the noise $Y_T^I + Y_C$. Y_T^I is Poisson distributed with mean $\frac{N}{2} \sum_{j=1}^{k_T} p_T(jT + t_s)$ independent from Y_C . For CPNS in high-rate regime, we showed in Subsection III-D that Y_C , follows a Poisson distribution with rate $M \sim \mathcal{N}(k_1, k_2)$. Therefore, the additive noise is distributed as $Y_{IC} = Y_T^I + Y_C \sim \text{Poisson}(M')$ where $M' = \mathcal{N}(k'_1, k_2)$ and $k'_1 = k_1 + \frac{N}{2} \sum_{j=1}^{k_T} p_T(jT + t_s)$. Therefore, we have

$$p_{Y_{IC}}[k] = \int_0^{+\infty} p_{Y_{IC}}[k|m] f_{M'}(m) dm, \quad (39)$$

where $p_{Y_{IC}}[k|m] = \frac{e^{-m} m^k}{k!}$ and $f_{M'}(m) = (2\pi k_2)^{1/2} \exp\left(-\frac{(m-k'_1)^2}{2k_2}\right)$. It is easy to see that $p_{Y_{IC}}[k|m]$ is a log-concave distribution in terms of (k, m) , and $f_{M'}(m)$ is log-concave distribution in terms of m . Since, pointwise multiplication of two log-concave functions is log-concave [31], joint distribution of (Y_{IC}, M') , i.e., $p_{Y_{IC}}[k|m] f_{M'}(m)$, is log-concave. Moreover, the marginal distributions of log-concave joint distribution is a log-concave distribution [31]. Therefore, $p_{Y_{IC}}[k]$ is a log-concave distribution. On the other hand, the optimal ML detector of the presence of signal embedded in the additive log-concave noise is a single-threshold detector [36]. \square

Now, we derive the BER of DMC system in the presence of CPNS in high-rate regime. Obviously, given $B_0 = b_0$, $Y = Y_T^I + Y_T^I + Y_C$ is a Poisson RV whose mean is $M'' = M + Nb_0 p_T(t_s) + \frac{N}{2} \sum_{j=1}^{k_T} p_T(jT + t_s)$. Since, $M \sim \mathcal{N}(k_1, k_2)$, we have $M'' \sim \mathcal{N}(k''_1, k_2)$ in which $k''_1 = k_1 + Nb_0 p_T(t_s) + \frac{N}{2} \sum_{j=1}^{k_T} p_T(jT + t_s)$. Considering (27), we can write

$$p_Y[k|B_0 = b_0] = l(k''_1, k_2) k_2^{(k+1)/2} D_{-k-1} \left(\sqrt{k_2} \left(1 - \frac{k''_1}{k_2} \right) \right). \quad (40)$$

Therefore, given a STD with threshold ζ , error probability is given by

$$P_e = \frac{1}{2} \left(1 - \mathcal{F}_Y(\zeta | B_0 = 0) \right) + \frac{1}{2} \mathcal{F}_Y(\zeta | B_0 = 1), \quad (41)$$

where $\mathcal{F}_Y(\cdot)$ denotes the cumulative distribution function (CDF) of RV Y whose pdf is given by (40). To obtain the optimal threshold value, one should minimize BER in terms of ζ . The following simple lemma concludes that when STD is an optimal ML detector, the corresponding BER is quasiconvex. Therefore, a bisection method [31] can be employed to obtain the optimal threshold value.

Lemma 1. *The optimal ML detector in (34) is single-threshold with optimal threshold ζ_o , if and only if the BER in (36) is a quasiconvex function of the threshold with global minimum at ζ_o .*

Proof. The proof is provided in Appendix C. □

Corollary 1. Obviously, when the BER is not a quasiconvex function of ζ , it has multiple local minimum and maximum points at $\zeta_1, \zeta_2, \dots, \zeta_m$ characterizing optimal MTD.

Optimality of STD in special case of large values of λ_e is borrowed from the log-concavity of normal distribution of M that results the log-concavity of Y_C . But, in the general case of CPNS, our results indicate that distributions of M and then $Y_C \sim \text{Poisson}(M)$ may not be log-concave and may even be multimodal in some conditions. Thereby, the distributions of received signals given $b_0 = 0$, and 1 in (33) may have multiple intersection points and correspondingly leading to optimality of a MTD (and not a STD). Fig. 3 (Left) depicts the logarithm of distribution of noise Y_C obtained based on simulation, where $N = 2 \times 10^5$, $T = 0.2$, $d_T = 10 \mu m$, $d_C = 5.5 \mu m$, $\lambda_a = 5 \times 10^5$, $\lambda_e = 15$, $r_R = 2.2 \mu m$. It is obvious that it is not a concave curve and then the logarithm of distribution of noise is not a log-concave distribution. Correspondingly, Fig. 3 (Right) shows the distributions of the number of received molecules given the transmission of bits 1 and 0 in the current time slot, i.e., $p_Y[k | B_0 = 1]$ and $p_Y[k | B_0 = 0]$ given by (33), respectively. It is observed that these two distributions are bimodal and have 3 intersection points and then optimal ML detector has 4 decision making regions which results in a MTD.

Remark 1. *Based on our vast numerical and simulation results, this phenomena rarely occurs for considered MC system in the presence of CPNS and is only theoretically of interest. Note that*

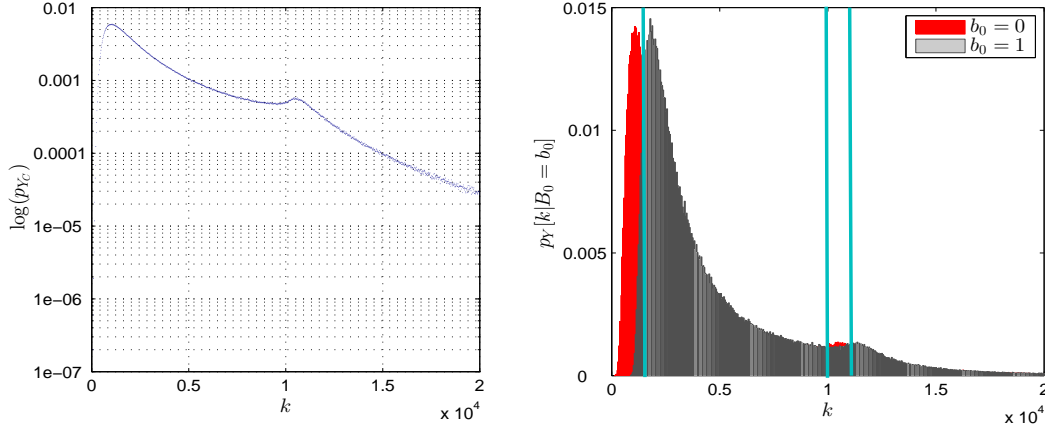


Fig. 3. (Left) The Logarithm of CPNS noise distribution. (Right) The received signal distribution given transmission of bits 0 and 1.

even for such rare scenarios, the difference between BER of the suboptimal STD and optimal MTD would be negligible, as it is deduced from Fig. 3.

V. NUMERICAL AND SIMULATION RESULTS

In this section, we evaluate the performance of the point-to-point DMC system in the presence of a CPNS. The DMC system parameters adopted for the analytical and simulation are given in Table V.

Fig. 4 shows the BER of the DMC system in the presence of a CPNS as a function of the time interval \tilde{T} used for the rare-event analysis obtained based on (i) the rare-event exact analysis given in (17), (ii) the rare-event approximate analysis given in (20), and (iii) simulation of 10^6 bits. The distance between the CPNS and the receiver and the corresponding channel memory are $d_C = 8 \mu m$ and $k_C = 10$, respectively. The event amplitude of the CPNS, which we refer to as the CPNS amplitude, is set to $\lambda_a = 10^5$. The BER curves are plotted for two different CPNS rates, $\lambda_e = 2$ and 10. We observe that both approximation and exact analytical results approach the simulation results for sufficiently short time intervals \tilde{T} for which rare-event property holds ($\lambda_e \tilde{T} \ll 1$).

Fig. 5 compares the BERs of the DMC system for a CPNS (the rare-event approximate analysis) and a homogeneous Poisson noise [12]. For a higher accuracy of rare-event analysis for the CPNS, we used very small value of $\tilde{T} = 0.002$. To have a fair comparison, the average mean of the homogeneous Poisson noise received in the current time slot, denoted by λ_0 , is set equal to the average number of molecules received from the CPNS in the current time slot, i.e.,

TABLE I
DMC SYSTEM PARAMETERS USED IN SIMULATIONS

Parameter	Variable	Value
Diffusion coefficient	D	$1.14 \times 10^{-9} \text{ m}^2/\text{sec}$
Time-slot duration	T	0.5, 0.1, and 0.02 sec
Number of transmitted molecules for bit '1'	N	0.5×10^5
Distance between transmitter and receiver	d_T	$4 \mu\text{m}$
Distance between CPNS and receiver	d_C	6, 8, and $12 \mu\text{m}$
Transmitter channel memory	k_T	10
CPNS channel memory	k_C	15
CPNS release time rate	$\lambda_e \tilde{T}$	0.001, 0.01, 0.1, 0.25 and 0.5
CPNS release amplitude rate	λ_a	8×10^6 , 10^5 , and 2×10^4
Receiver radius	r_R	$0.5 \mu\text{m}$

$$\hat{\lambda}_0 = \sum_{n=0}^{\infty} \int_{\theta_{1:n}} \lambda_a \sum_{i=1}^n p_C(k_C T - \theta_i) f_{\theta}(\theta_{1:n}) p_{N_e}[n] d\theta_{1:n}. \quad (42)$$

The BER is depicted versus the threshold value ζ for $\lambda_e = 0.5$ and $\lambda_e = 5$. We used $d_C = 8 \mu\text{m}$. Fig. 5 reveals that assuming a homogeneous Poisson noise at the receiver leads to an overly optimistic performance prediction when the noise source is actually a CPNS. Therefore, homogeneous Poisson noise models are not capable of modeling CPNSs. Furthermore, a CPNS with a lower rate ($\lambda_e = 0.5$), results in a higher performance than a CPNS with a higher rate ($\lambda_e = 5$), as expected. Also, it is observed that the simulation results confirm the provided analysis.

Fig. 6 shows the BER of the DMC system in the presence of a CPNS in low and moderate rate regime ($\lambda_e = 0.5, 5, 10$) versus threshold ζ , for various parameters including λ_a , N , and d_C . The rare-event approximation analysis was used. The distance between the transmitter and the receiver is fixed to $d_T = 4 \mu\text{m}$. For all five considered scenarios, the BER is a quasiconvex function of ζ , and considering Lemma 1, the optimal detector is a simple STD.

Fig. 8 compares the distribution of $M = \lambda_a \sum_{i=1}^{N_e} p_C(k_C T - \Theta_i)$ obtained based on the simulation with normal distribution approximation $\mathcal{N}(k_1, k_2)$ given in (25), for different values of λ_e . It is observed that the distribution of M approaches the normal distribution for high values of λ_e ($\lambda_e > 100$), confirming our analysis provided in Section III.D. Correspondingly, Fig. 9 depicts the BER of the DMC system in the presence of a CPNS versus λ_e obtained based on simulation and analysis given in (41) which employs normal approximation of $\mathcal{N}(k_1, k_2)$, for

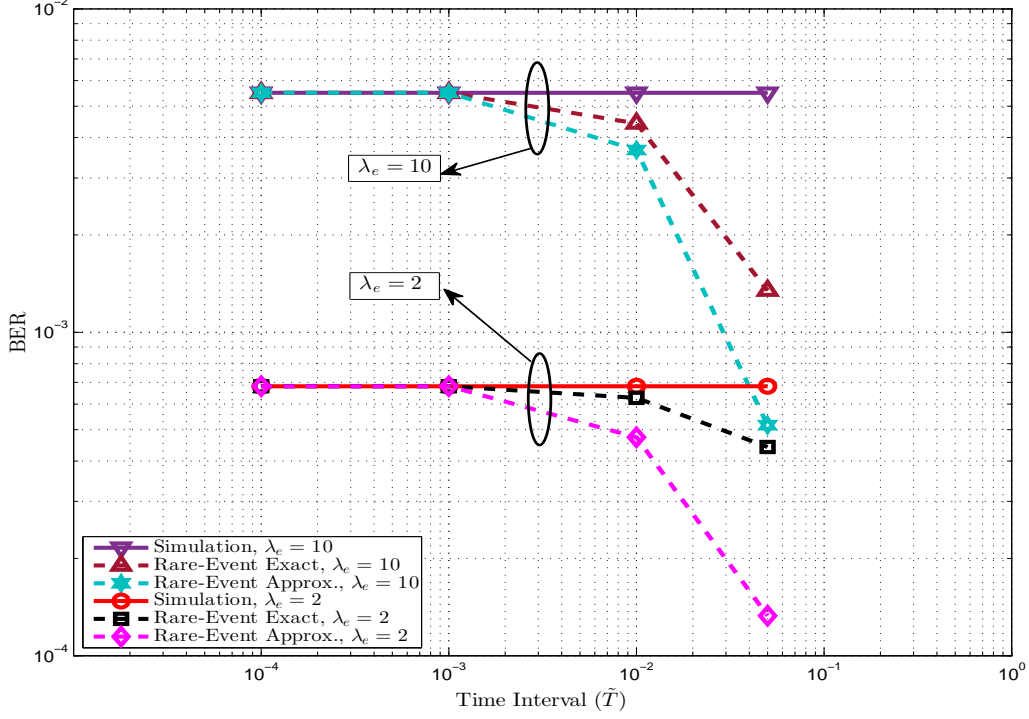


Fig. 4. Comparison of BERs (exact, approximation, and simulation) versus time interval \tilde{T} for different values of λ_e .

different values of $T = 0.02, 0.1$. It is observed that the simulation results coincide our analysis for high values of λ_e ($\lambda_e > 100$). Moreover, we observe that BER increases by increasing λ_e .

Fig. 7 depicts the BER of the DMC system versus λ_a for different values of $d_C = 6, 9, 12 \mu m$. As expected, by increasing the distance of the CPNS from the receiver, d_C , the BER decreases which results in a better performance. For small values of λ_a such as $\lambda_a \leq 10^3$, the performance is approximately the same for all distances as the impact of the CPNS on the performance of the point-to-point link becomes negligible for extremely low λ_a s. In this case, the randomness of the diffusion channel between the transmitter and receiver is the dominant effect on performance. On the other hand, when we have higher λ_a values, sensitivity of BER to both values of λ_a and d_C increases.

VI. CONCLUSION

In this paper, impact of the presence of biological organs in in-vivo environment as external noise source for DMC system was investigated. The release of molecules by a biological noise source was modeled as a CPP. A point-to-point DMC link in the presence of a CPNS was considered. The distribution of the number of molecules received from CPNS was analyzed

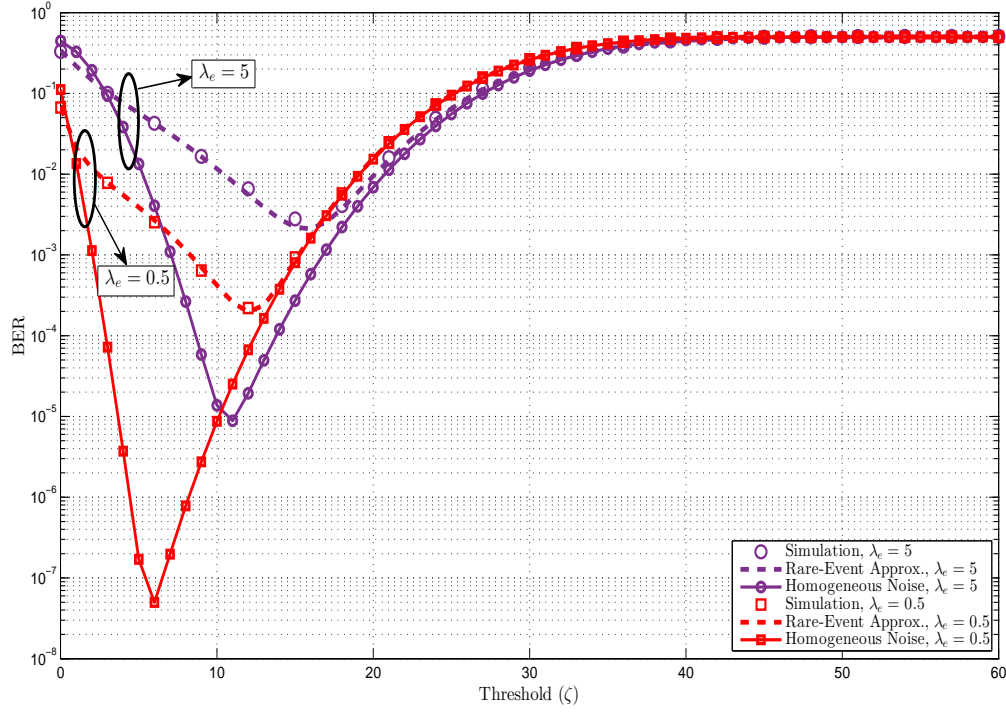


Fig. 5. BER of the DMC system in the presence of a CPNS. The BER is obtained based on the rare-event approximation compared to the homogeneous Poisson noise assumption.

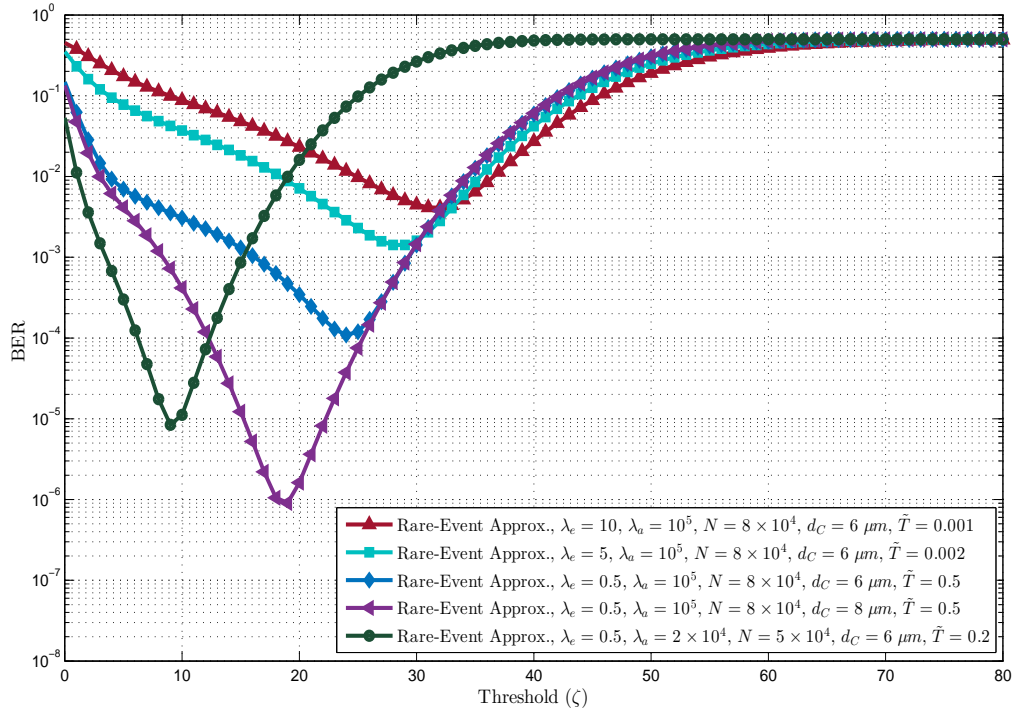


Fig. 6. BER of the DMC system in the presence of a CPNS employing the rare-event approximation analysis.

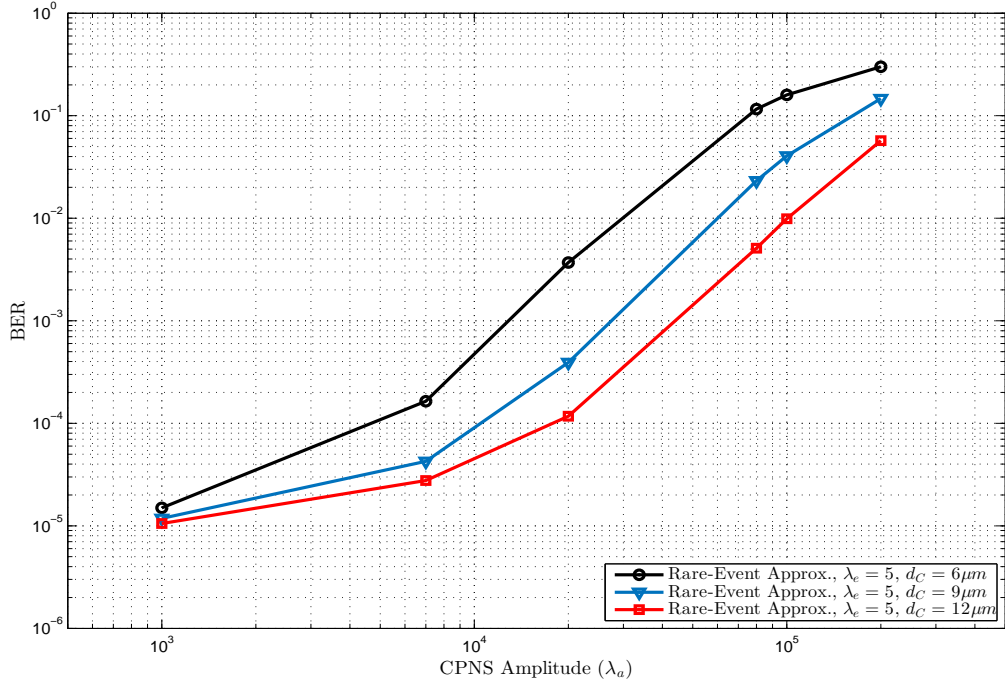


Fig. 7. BER of the DMC system in the presence of a CPNS versus λ_a for various distances $d_C = 6, 9, 12 \mu m$.

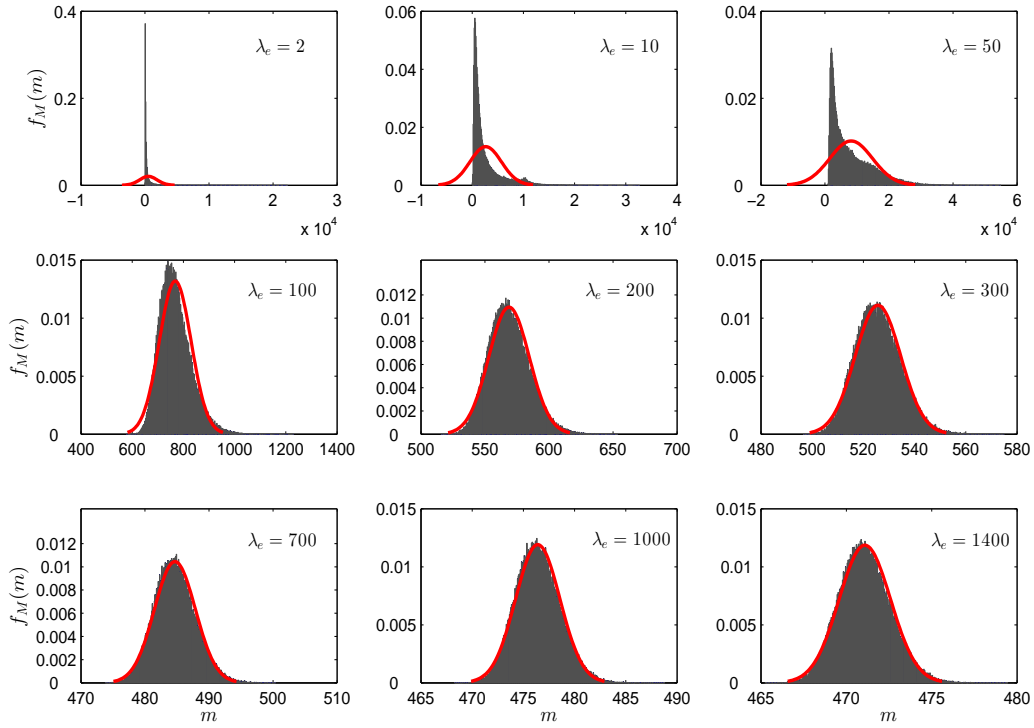


Fig. 8. Comparison of distribution of $M = \lambda_a \sum_{i=1}^{N_e} p_C(k_C T - \Theta_i)$ obtained from simulation with normal approximation $\mathcal{N}(k_1, k_2)$ for various λ_e .

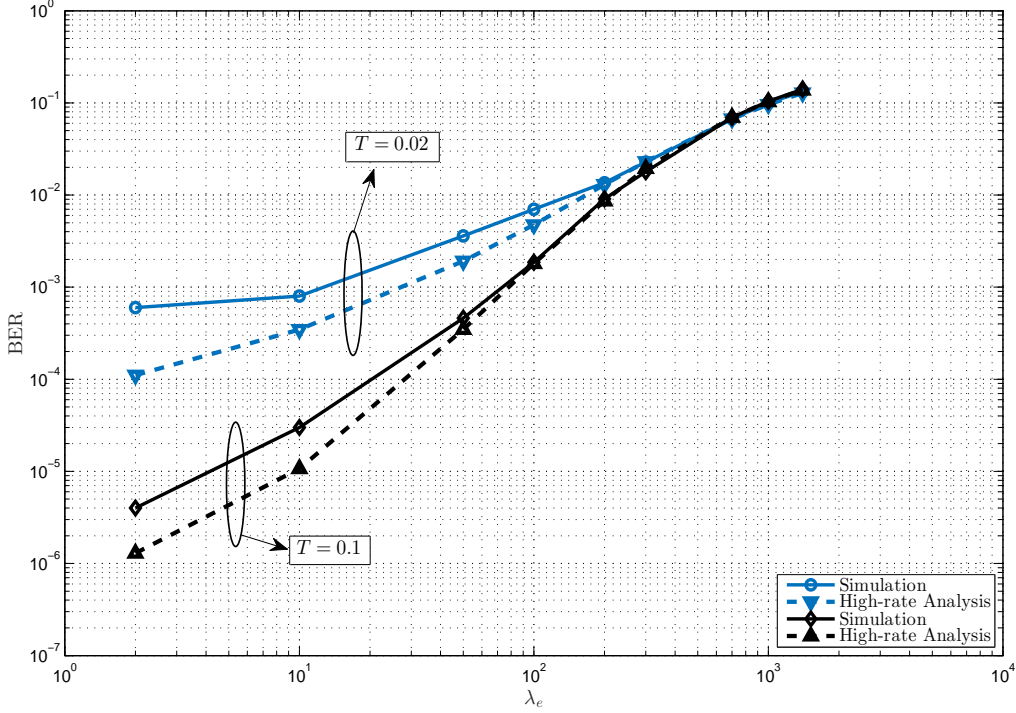


Fig. 9. BER of the DMC system versus λ_e obtained based on simulation and high-rate analysis.

based on the rare event distribution and shown to be a Poisson mixture distribution. Assuming a simple on-off keying modulation, symbol-by-symbol ML detector was formulated and BER was analyzed in closed-form expressions. For special case of CPNS in high-rate regime, the noise received from the CPNS is approximated by a Poisson process whose rate is normal distributed. It was proved that the optimal ML detector is a simple STD, for CPNS in high rate regime. However, our results revealed that STD may not be the optimal ML detector, in the general case of CPNS. Moreover, based on our results, presented model and analysis for the DMC system performance in the presence of a CPNS is necessary and simply adopting conventional homogeneous Poisson noise model may lead to overly optimistic performance predictions. This new type of noise source introduces new molecular communication channel with properties different from conventional MC channels that should be investigated from various perspectives.

APPENDIX A

EQUIVALENCE OF (14) AND (17)

It is straightforward to see that (14) and (17) are equivalent. For simplicity of presentation, we show this equivalence for the special case of $\tilde{k}_C = 3$. Starting from (14), for $\tilde{k}_C = 3$ we

have:

$$p_{Y_C}[k] = p_{\tilde{Y}_C^1}[k] \otimes p_{\tilde{Y}_C^2}[k] \otimes p_{\tilde{Y}_C^3}[k], \quad (43)$$

Substituting $p_{\tilde{Y}_C^1}[k]$, $p_{\tilde{Y}_C^2}[k]$, and $p_{\tilde{Y}_C^3}[k]$ by (16) and employing $f_i[k] = p_{\tilde{Y}_C^i}[k|\mathcal{F}_1]$, we obtain:

$$\begin{aligned} p_{Y_C}[k] &= ((1 - \lambda_e \tilde{T})\delta[k] + \lambda_e \tilde{T} f_1[k]) \otimes ((1 - \lambda_e \tilde{T})\delta[k] + \lambda_e \tilde{T} f_2[k]) \otimes ((1 - \lambda_e \tilde{T})\delta[k] + \lambda_e \tilde{T} f_3[k]) \\ &= (1 - \lambda_e \tilde{T})^3 \delta[k] + (1 - \lambda_e \tilde{T})^2 (\lambda_e \tilde{T}) (f_1[k] + f_2[k] + f_3[k]) + (1 - \lambda_e \tilde{T}) (\lambda_e \tilde{T})^2 (f_1[k] \otimes f_2[k] \\ &\quad + f_1[k] \otimes f_3[k] + f_2[k] \otimes f_3[k]) + (\lambda_e \tilde{T})^3 (f_1[k] \otimes f_2[k] \otimes f_3[k]) \end{aligned} \quad (44)$$

which can be rewritten as follows:

$$\begin{aligned} p_{Y_C}[k] &= (1 - \lambda_e \tilde{T})^3 \delta[k] + (1 - \lambda_e \tilde{T})^2 (\lambda_e \tilde{T}) \sum_{h=1}^3 \delta[k] \otimes f_{\alpha_1^h}[k] \\ &\quad + (1 - \lambda_e \tilde{T}) (\lambda_e \tilde{T})^2 \sum_{h=1}^3 \delta[k] \otimes f_{\alpha_1^h}[k] \otimes f_{\alpha_2^h}[k] + (\lambda_e \tilde{T})^3 (\delta[k] \otimes f_{\alpha_1^1}[k] \otimes f_{\alpha_2^1}[k] \otimes f_{\alpha_3^1}[k]) \quad (45) \\ &= \sum_{i=0}^3 (1 - \lambda_e \tilde{T})^{3-i} (\lambda_e \tilde{T})^i \sum_{h=1}^{\mathfrak{K}_i} \delta[k] \otimes f_{\alpha_1^h}[k] \otimes \cdots \otimes f_{\alpha_i^h}[k]. \end{aligned}$$

where $\mathfrak{K}_i \triangleq \binom{3}{i}$. This completes the proof.

APPENDIX B

DERIVING CLOSED-FORM EXPRESSION FOR $p_{Y_C}[k]$ IN THE HIGH-RATE REGIME

From (26), we have:

$$\begin{aligned} p_{Y_C}[k] &= \int_0^{+\infty} e^{-m} \frac{m^k}{k!} (2\pi k_2)^{-1/2} \exp\left(-\frac{(m - k_1)^2}{2k_2}\right) dm \\ &= \frac{(2\pi k_2)^{-1/2}}{k!} \int_0^{+\infty} m^k \exp\left(-m - \frac{(m - k_1)^2}{2k_2}\right) dm \\ &= \frac{(2\pi k_2)^{-1/2}}{k!} e^{-k_1^2/k_2} \int_0^{+\infty} m^k \exp\left(-\frac{m^2}{2k_2} - \left(1 - \frac{k_1}{k_2}\right)m\right) dm. \end{aligned} \quad (46)$$

By changing variable $m = (2k_2)^{1/2}x$, we obtain

$$p_{Y_C}[k] = \frac{(2\pi k_2)^{-1/2}}{k!} e^{-k_1^2/k_2} (2k_2)^{(k+1)/2} \int_0^{+\infty} x^k \exp\left(-x^2 - \sqrt{2k_2}\left(1 - \frac{k_1}{k_2}\right)x\right) dx. \quad (47)$$

On the other hand we have the following integral [34], [35]:

$$\int_0^{+\infty} x^\nu e^{-x^2 - \gamma x} dx = 2^{-(\nu+1)/2} \Gamma(\nu+1) e^{\gamma^2/8} D_{-\nu-1}(\gamma/\sqrt{2}). \quad (48)$$

Substituting $\gamma = \sqrt{2k_2}(1 - \frac{k_1}{k_2})$ and $\nu = k$ into (48) and applying the result in (47), (27) is resulted.

APPENDIX C

THE PROOF FOR LEMMA 1

Given a STD with the threshold value of ζ , the BER of the system is given by (36). Therefore, we have

$$\frac{\partial P_e}{\partial \zeta} = \frac{1}{2} \left(p_Y[\zeta|B_0 = 1] - p_Y[\zeta|B_0 = 0] \right). \quad (49)$$

First we provide the direct proof, i.e., if optimal ML detector in (34) is STD with optimal threshold ζ_o , P_e in (36) is necessarily quasiconvex function of ζ with global minimum at ζ_o . Assume that the optimal ML detector is a STD, where the optimal threshold value is ζ_o . Considering (34) and (35), we can write $1 = \arg\max_{b_0} p_Y[\zeta|B_0 = b_0]$, for all $\zeta > \zeta_o$ and $0 = \arg\max_{b_0} p_Y[\zeta|B_0 = b_0]$, for all $\zeta < \zeta_o$. Equivalently, we have $p_Y[\zeta|B_0 = 1] \geq p_Y[\zeta|B_0 = 0]$ and $p_Y[y|B_0 = 1] \leq p_Y[\zeta|B_0 = 0]$ for all $\zeta > \zeta_o$ and $\zeta < \zeta_o$, respectively. Therefore, we can write $p_Y[\zeta|B_0 = 1] - p_Y[\zeta|B_0 = 0] \geq 0$ and $p_Y[\zeta|B_0 = 1] - p_Y[\zeta|B_0 = 0] \leq 0$ for all $\zeta > \zeta_o$ and $\zeta < \zeta_o$, respectively. Regarding to (49), $\partial P_e / \partial \zeta$ is positive and negative for $\zeta > \zeta_o$ and $\zeta < \zeta_o$, respectively. Equivalently, P_e is decreasing function for $\zeta < \zeta_o$ and increasing for $\zeta > \zeta_o$. Thereby, P_e is a quasiconvex function of ζ which has a global minimum at ζ_o .

Now, we provide the converse proof, i.e., if BER given in (36) is quasiconvex function of ζ with global minimum at ζ_o , the optimal ML detector in (34) is a STD with optimal threshold ζ_o : Assuming P_e given in (36) is quasiconvex of ζ with a global minimum at ζ_o , $\partial P_e / \partial \zeta$ is positive and negative for all $\zeta > \zeta_o$ and $\zeta < \zeta_o$, respectively. Therefore, we have $p_Y[\zeta|B_0 = 1] - p_Y[\zeta|B_0 = 0] \geq 0$ and $p_Y[\zeta|B_0 = 1] - p_Y[\zeta|B_0 = 0] \leq 0$ for $\zeta > \zeta_o$ and $\zeta < \zeta_o$, respectively, considering (49). Equivalently, $p_Y[\zeta|B_0 = 1] \geq p_Y[y|B_0 = 0]$ and $p_Y[\zeta|B_0 = 1] \leq p_Y[y|B_0 = 0]$ for all $\zeta > \zeta_o$ and $\zeta < \zeta_o$, respectively. Therefore, we can write $0 = \arg\max_{b_0} p_Y[\zeta|B_0 = b_0]$, for $\zeta < \zeta_o$ and $1 = \arg\max_{b_0} p_Y[\zeta|B_0 = b_0]$, for $\zeta > \zeta_o$ which is equivalent to optimality of STD with threshold ζ_o , considering (34) and (35).

REFERENCES

- [1] Akyildiz, Ian F., Fernando Brunetti, and Cristina Blázquez, "Nanonetworks: A new communication paradigm," *Computer Networks*, vol. 52, no. 12, pp. 2260-2279, Aug. 2008.
- [2] M. Pierobon and I. Akyildiz, "A physical end-to-end model for molecular communications in nanonetwork," *IEEE Journal on Selected Areas in Communications*, vol. 28, no. 4, pp. 602-611, May 2010.
- [3] I. Akyildiz, M. Pierobon, S. Balasubramaniam, and Y. Koucheryavy, "The internet of bio-nano things," *IEEE Communications Magazine*, vol. 53, no. 3, pp. 32-40, Mar. 2015.
- [4] B. Atakan, O. B. Akan, and S. Balasubramaniam, "Body area nanonetworks with molecular communications in nanomedicine," *IEEE Communications Magazine*, vol. 50, no. 1, pp. 28-34, Jan. 2012.
- [5] Y. Chahibi, M. Pierobon, S. O. Song, and I. F. Akyildiz, "A molecular communication system model for particulate drug delivery systems," *IEEE Transactions on Biomedical Engineering*, vol. 60, no. 12, pp. 3468-3483, Dec. 2013.
- [6] P. M. Conn, M. L. Johnson, and J. D. Veldhuis, *Quantitative Neuroendocrinology*, Vol. 28. Academic Press, 1995.
- [7] D. M. Keenan, and J. D. Veldhuis, "Stochastic model of admixed basal and pulsatile hormone secretion as modulated by a deterministic oscillator," *American Journal of Physiology-Regulatory, Integrative and Comparative Physiology*, vol. 273, no. 3, pp. 1182-1192, Sep. 1997.
- [8] S. B. Lowen, S. S. Cash, M. M. Poo, and M. C. Teich, "Quantal neurotransmitter secretion rate exhibits fractal behavior", *Journal of neuroscience*, vol. 17, no. 15, pp. 5666-5677, Aug. 1997.
- [9] H. Arjmandi, A. Ahmadzadeh, R. Schober, and M. N. Kenari, "Ion channel based bio-synthetic modulator for diffusive molecular communication," *IEEE Transactions on Nanobioscience*, vol. 15, no. 5, pp. 418-432, Jul. 2016.
- [10] M. Pierobon and I. F. Akyildiz, "Diffusion-based noise analysis for molecular communication in nanonetworks," *IEEE Transactions on Signal Processing*, vol. 59, no. 6, pp. 2532-2547, Jun. 2011.
- [11] K. V. Srinivas, A. Eckford, and R. Adve, "Molecular communication in fluid media: The additive inverse gaussian noise channel," *IEEE Transactions on Information Theory*, vol. 58, no. 7, pp. 4678-4692, Jul. 2012.
- [12] H. Arjmandi, A. Gohari, M. Nasiri-Kenari, and F. Bateni, "Diffusion based nanonetworking: A new modulation technique and performance analysis," *IEEE Communications Letters*, vol. 17, no. 4, pp. 645-648, Apr. 2013.
- [13] N. Farsad, W. Guo, C. B. Chae, and A. Eckford, "Stable distributions as noise models for molecular communication," in *IEEE Global Communications Conference (GLOBECOM)*, pp. 1-6, Dec. 2015.
- [14] A. Singhal, R. K. Mallik, and B. Lall, "Effect of molecular noise in diffusion-based molecular communication," *IEEE Wireless Communications Letters*, vol. 3, no. 5, pp. 489-492, Oct. 2014.
- [15] A. Einolghozati, M. Sardari, and F. Fekri, "Capacity of diffusion-based molecular communication with ligand receptors," in *Information Theory Workshop (ITW)*, pp. 85-89, Oct. 2011.
- [16] B. Atakan, "Passive molecular communication through ligand-receptor binding," in *Molecular Communications and Nanonetworks*, Springer New York, 2014.
- [17] G. Aminian, M. Farahnak-Ghazani, M. Mirmohseni, M. Nasiri-Kenari, and F. Fekri, "On the capacity of point-to-point and multiple-access molecular communications with ligand-receptors," *IEEE Transactions on Molecular, Biological and Multi-Scale Communications*, vol. 1, no. 4, pp. 331-346, Dec. 2015.

- [18] R. Mosayebi, H. Arjmandi, A. Gohari, M. Nasiri-Kenari, and U. Mitra, "Receivers for diffusion-based molecular communication: Exploiting memory and sampling rate," *IEEE Journal of Selected Areas in Communications*, vol. 32, no. 12, pp. 2368-2380, Dec. 2014.
- [19] L. Felicetti, M. Femminella, G. Reali, T. Nakano, and A. V. Vasilakos, "TCP-like molecular communications," *IEEE Journal on Selected Areas in Communications*, vol. 32, no. 12, pp. 2354-2367, Dec. 2014.
- [20] A. Ahmadzadeh, A. Noel, and R. Schober, "Analysis and design of multi-hop diffusionbased molecular communication networks," *IEEE Transactions on Molecular Biological, and Multi-Scale Communications*, vol. 1, no. 2, pp. 144-157, Jun. 2015.
- [21] F. B. Hanson, *Applied stochastic processes and control for Jump-diffusions: modeling, analysis, and computation*, vol. 13, Siam, 2007.
- [22] J. Philibert, "One and a half century of diffusion: Fick, Einstein, before and beyond," *Diffusion Fundamentals*, vol. 4, no. 6, pp. 1-19, 2006.
- [23] M. U. Mahfuz, D. Makrakis, and H. T. Mouftah, "A comprehensive study of sampling-based optimum signal detection in concentration-encoded molecular communication," *IEEE Transactions on NanoBioscience*, vol. 13, no. 3, pp. 208-222, Sep. 2014.
- [24] M. Pierobon, I. F. Akyildiz, "Capacity of a diffusion-based molecular communication system with channel memory and molecular noise," *IEEE Transactions on Information Theory*, vol. 59, no. 2, pp. 942-954, Feb. 2013.
- [25] J. Grandell, *Mixed poisson processes*. CRC Press, 1997.
- [26] D. J. Daley, D. Vere-Jones, *An introduction to the theory of point processes: volume II: general theory and structure*. Springer Science and Business Media, Nov. 2007.
- [27] J. Keilson, *Markov chain models—rarity and exponentiality*. Springer Science & Business Media, 2012.
- [28] D. Karlis, E. Xekalaki, "Mixed poisson distributions," *International Statistical Review*, vol. 73, no. 1, pp. 35-58, Apr. 2005.
- [29] J. Shao, *Mathematical statistics*, Second Edition, Springer Science, 2007.
- [30] S. M. Kay, *Fundamentals of Statistical Signal Processing: Estimation Theory*. Prentice Hall, 1993.
- [31] S. Boyd, L. Vandenberghe. *Convex optimization*. Cambridge university press, 2004.
- [32] S. O. Rice, "Mathematical analysis of random noise," *Bell Labs Technical Journal*, vol. 23, no. 3, July 1944.
- [33] S. B. Lowen, and M. C. Teich, "Power-law shot noise," *IEEE Transactions on Information Theory*, vol. 36, no. 6, pp. 1302-1318, Nov. 1990.
- [34] V. H. Moll, *Special integrals of Gradshteyn and Ryzhik: the proofs*. Vol. 2. CRC Press, 2015.
- [35] A. Winkelbauer, "Moments and absolute moments of the normal distribution," arXiv preprint arXiv:1209.4340, Sep. 2012.
- [36] P. Prucnal, and M. Teich. "Single-Threshold Detection of a Random Signal in Noise with Multiple Independent Observations, Part 2: Continuous Case." *IEEE Transactions on Information Theory*, vol. 25, no .2, pp. 213-218, Mar. 1979.